ROYAL SOCIETY
OF CHEMISTRY

RESEARCH ARTICLE

Check for updates

Antibacterial peptidomimetics based on guanidine-functionalized di-tertiary amides

Ghayah Bahatheg, [iD] *[ab] Rajesh Kuppusamy,*[ac] Lissy M. Hartmann,[d] Charles G. Cranfield, [iD] [d] David StC. Black, [iD] [a] Mark Willcox[c] and Naresh Kumar [iD] *[a]

Tertiary amides such as peptoids are a novel class of peptidomimetics that offer enhanced structure, activity, and stability compared to many naturally occurring antimicrobial peptides. Guanidino compounds have gained interest in medicinal chemistry as cell-penetrating molecules. This work investigates the changes in the antibacterial activity of modified guanidino groups on the structure of active guanidino tertiary amides by incorporating lipophilic, hydrophobic, and extra cationic groups, thereby combining the properties of the tertiary amide in the peptoid backbone with the important role of addition of extra cationic and lipophilic residues, such as those in AMPs, but supported by guanidine backbones. A library of active antibacterial bromo-phenyl and dichloro-phenyl-based guanidinium tertiary amides, including three series, was designed. These compounds exhibited MICs of 1–2 µg mL^{-1}, 4–8 µg mL^{-1}, and 16.5–35.6 µg mL^{-1} against *S. aureus*, *E. coli*, and *P. aeruginosa*, respectively. Tertiary amides with their guanidine bearing an alkylated cationic group of 3C (**19a** and **20a**) and 6C (**19b** and **20b**) length resulted in the most active molecules against all tested strains. Additionally, at 8× MIC, compound **19b** was the most effective *S. aureus* biofilm disruptor, disrupting 75% of the biofilm, while compound **19g** was the most active molecule against *E. coli* biofilm, with 50% disruption. The membrane permeability and QCM-D studies suggested that the designed cationic tertiary amides could depolarize and disrupt the bacterial cell membrane. The most potent peptoids were non-toxic, with HC$_{50}$ of more than 50 µg mL^{-1}.

Introduction

New classes of antibacterial drugs are in urgent demand to stem the extreme resistance of pathogenic bacterial cells against conventional antibiotics, which is negatively affecting the progress of therapeutic accomplishments.[1,2] The World Health Organization has classified resistance to traditional antibiotics as one of the three major public health threats in the 21st century.[1] Traditional antibiotics generally act on specific cellular targets, providing sufficient time for the development of unpredictable resistance. Additionally, bacterial biofilms enhance bacterial resistance and are particularly challenging for traditional antibiotics to overcome.[3]

[a] School of Chemistry, The University of New South Wales (UNSW), Sydney, NSW 2052, Australia. E-mail: g.bahatheg@unsw.edu.au, r.kuppusamy@unsw.edu.au, n.kumar@unsw.edu.au
[b] Department of Chemistry, Faculty of Science, University of Jeddah, Jeddah 21589, Saudi Arabia
[c] School of Optometry and Vision Science, The University of New South Wales (UNSW), Sydney, NSW 2052, Australia
[d] School of Life Sciences, University of Technology Sydney, PO Box 123, Ultimo 2007, Australia

Natural antimicrobial peptides (AMPs) have gained interest as alternatives to conventional antibiotics. Their structures are rich in cationic and hydrophobic residues, allowing them to quickly damage the anionic surface of microbial cytoplasmic membranes.[4] Despite AMPs showing unique antimicrobial potency against different pathogens, including bacteria, fungi, and viruses,[5,6] the clinical use of them is limited.[7] These limitations are due to their chemical instability, protease susceptibility, and sometimes poor permeability into the target cell membrane.[6,8] The chemical stability of the drugs is critical for localisation, efficacy, and safety. Here, the tertiary amides, as in peptoid-based scaffolds, can enhance the stability in the presence of protease action.[9]

Peptoids or *N*-substituted glycines are a class of peptidomimetics that with demonstrated activity against a broad spectrum of microbes.[7] This high potency of peptoids is due to their rigid tertiary amide structure (the side chain connected to nitrogen instead of alpha carbonyl carbon) compared to AMPs, which makes their structures chemically and physically stable.[7,10] These advantages of peptoids as tertiary amides bearing different cationic and/or hydrophobic residues have increased the attention of researchers to design more of these structures. Similarly, tertiary amide-based

fungicides such as isoflucypram, metalaxyl, benalaxyl, and ofurace have been commercialized.[11] Despite their potential, relatively few studies have explored the design and optimization of tertiary amide-based peptoid-inspired peptidomimetics for antibacterial applications. Salinomycins commonly used in veterinary medicine its tertiary amide derivatives showed good antibacterial activity against both Gram-positive and Gram-negative bacteria.[11]

Incorporating a guanidine group into molecules is a practical method to enhance antibacterial activity.[12] Insertion of guanidino (arginine-type) instead of amino (lysine-type) groups into antibacterial tertiary amide backbones of the peptoids improves their antibacterial properties.[13,14] Recently, guanidinium and lipophilic molecules have gained interest in medicinal chemistry as cellular delivery vehicles due to their cell-penetrating abilities.[13,15–19] The effectiveness of the guanidino group can be attributed to the delocalization of the charge of the guanidino group due to the resonance process, which increases the stability of the positive charge on the guanidine part, leading to an increase in the electrostatic interaction with bacterial membrane phospholipids.[20,21] Considering the potential of the guanidino group on the molecule activity, researchers have designed antibacterial compounds containing arginine-type monomers instead of lysine-type monomers 1 (Fig. 1).[22] The same group in a different study added more than ten different residues into their structures and reported that the best active compounds against a broad spectrum of Gram-positive and Gram-negative bacteria were guanidino derivatives (NhArg-Nmfp-Nmfp)$_4$ and (NhArg-Nphe-Nphe)$_4$.[23]

Lipophilicity is another feature that can help impart antibacterial activity by increasing the membrane permeability of the molecules.[24] Fatty acid residues are a fundamental factor in the potent activity of some antibiotics such as daptomycin and the polymyxin families.[25,26]

The attachment of a lipid tail to lysine-type compounds increased the antibacterial activity, and the most active compound was **MG10** (Fig. 1) attached to the longest lipid tail of 16C with an MIC of 6.3 μg mL^{-1} against S. aureus and E. coli.[27] Additionally, the antibacterial compound 1 H-(NLys-Nspe-Nspe)$_4$-NH$_2$ shows increased activity when fatty tails (Npent, Ndec, and Ntridec residues) are added, and the Ntridec-$_{14mer}$ lipopeptoid 2 (Fig. 1) with the longest lipophilic tail showed the most activity against B. subtilis with MIC of 1.8 μg mL^{-1} and an MIC on 14 μg mL^{-1} against E. coli.[28] Moreover, Ntridec-$_{14mer}$ lipidic molecule showed an ability to disrupt S. aureus and P. aeruginosa pre-established biofilms.[29,30] Other researchers have inserted alkyl chains with variable length to the sides and the centre of short antibacterial and antibiofilm compound 3 (Fig. 1), and shown that the length of the alkyl chains modulates antibacterial activity and mammalian cell toxicity.[31]

It has been reported that guanidino molecules have a higher antibacterial potential than other molecules.[32] In this work, active amino tertiary amides 12a and 12b[32,33] were subjected to a guanidination reaction using substituted guanidine reagents. The guanidine reagents were first prepared by i) directly connecting a lipophilic tail or aromatic group to the guanidine moiety, ii) thioureas containing a phenyl group and amino-alkyl or phenyl group, or iii) thioureas with an ethylamine and substituted phenyl moieties. These guanidine reagents were reacted with amino tertiary amides to give three different series (Fig. 2).

Results and discussion

Synthesis

Synthesis of the reagents. To design substituted guanidine derivatives, firstly, three series of reagents were synthesized (Schemes 1 and 2). The first series of reagents contained the
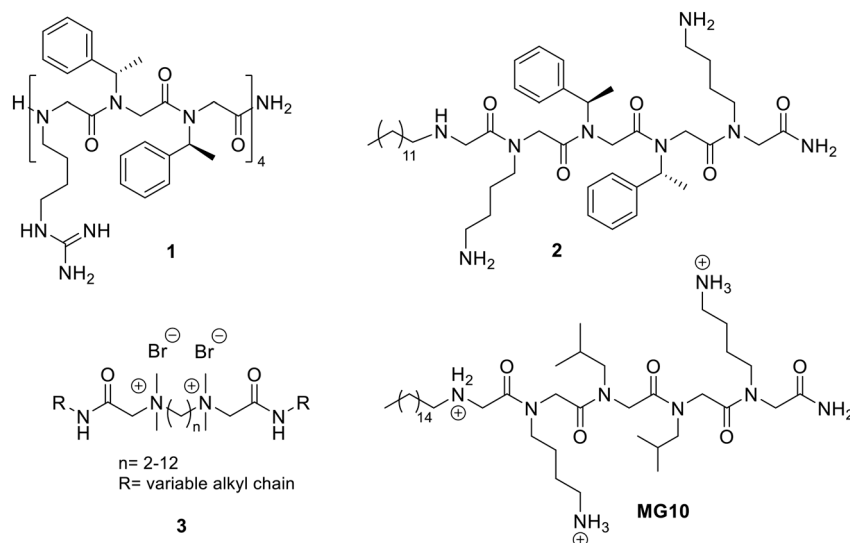

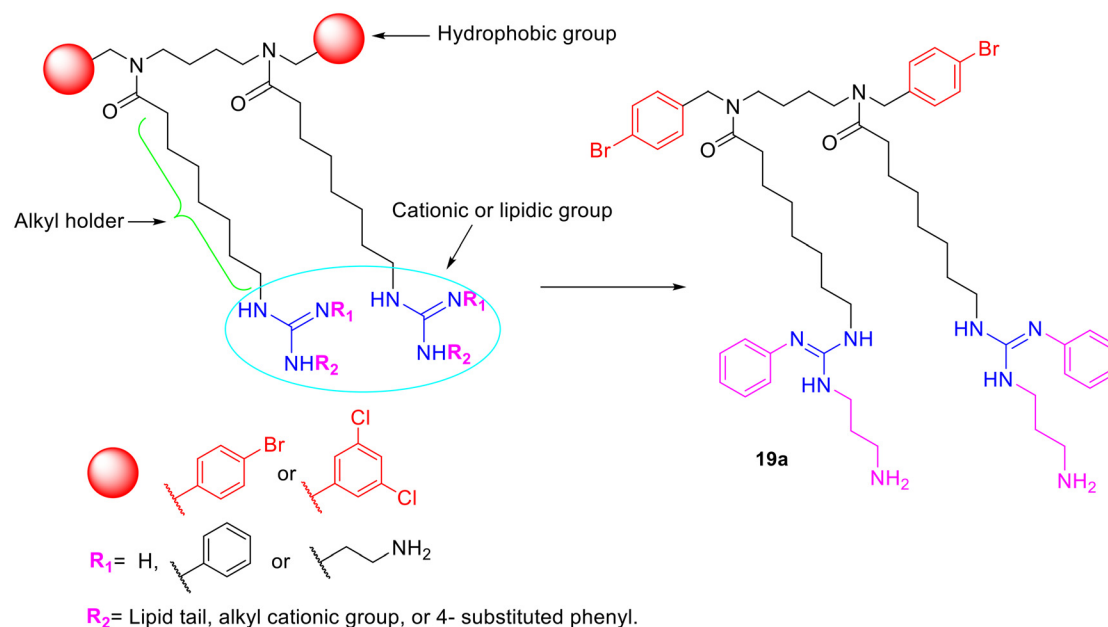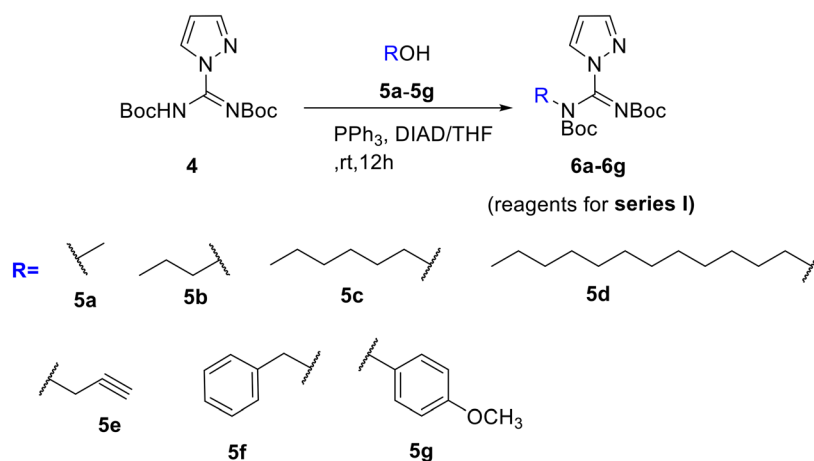**Fig. 1** Selected examples of guanidino and lipo-tertiary amides.

Fig. 2 General structures of modified guanidino tertiary amide.

Scheme 1 Synthesis of substituted carboxamidine reagents.

substituted carboxamidines. These reagents included different hydrophobic groups, such as lipid tails and aromatic moieties, to investigate the effect of the lipophilicity on the antibacterial activity.

To design the first series of the guanidine reagents, different alcohols **5a–5g** were added to *N,N′*-di-Boc-1*H*-pyrazole-1-carboxamidine under Mitsunobu reaction conditions to yield carboxamidine derivatives **6a–6g** (Scheme 1).
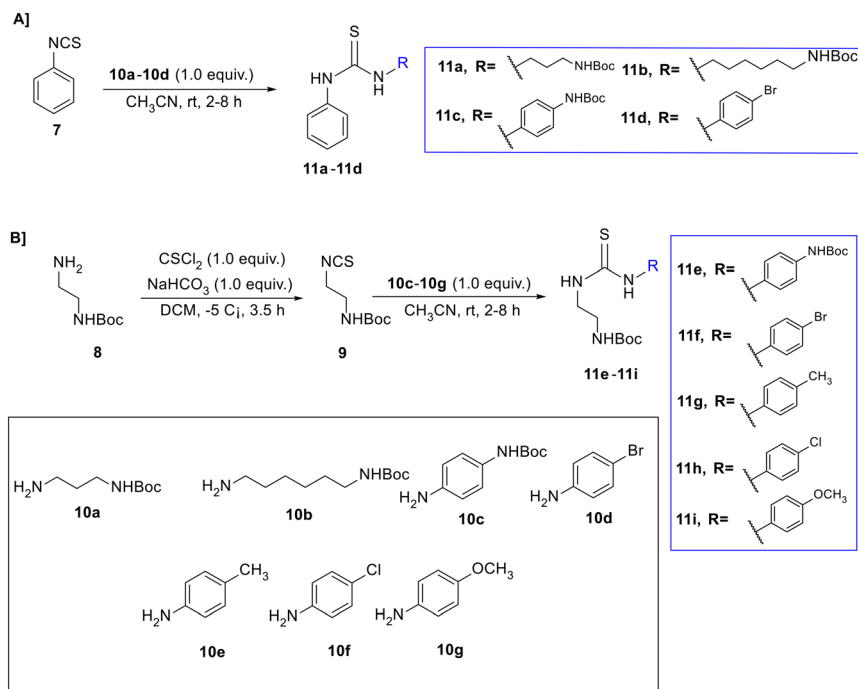
The second and third series were designed to create different thiourea reagents bearing one or two cationic sides and substituted or unsubstituted phenyl rings, in order to explore the effect of cationic and hydrophobic groups on the antibacterial activity. The second series was formed by adding different *N*-Boc-amino compounds **10a–10d** to phenyl isothiocyanate **7**, producing thiourea reagents **11a–11d** (Scheme 2A).

To synthesize the third series, first, compound *N*-Boc-ethylenedi-amine **8** was reacted with thiophosgene (CSCl$_2$) in the presence of sodium bicarbonate (NaHCO$_3$) and dichloromethane (DCM) as a solvent to produce *N*-Boc-ethylamine isothiocyanate **9**. This was followed by connecting compound **9** (cationic group) with the 4-substituted phenyl reagents (**10c–10g**) as hydrophobic groups to afford the thioureas **11e–11i** (Scheme 2B).

Synthesis of the lipophilic and cationic tertiary amide

To synthesize the first series of substituted guanidine tertiary amides, the amino tertiary amides **12a**[33] and **12b**[32] were reacted with compounds **6a–6g** to form the Boc-protected guanidino tertiary amides **13a–13g** and **14a–14g**. This was followed by the removal of the Boc group using

Scheme 2 Preparation of the substituted thiourea reagents, A] using phenyl isothiocyanate **7**, and B] using *N*-Boc-ethylamine isothiocyanate **9**.

trifluoroacetic acid in DCM, which gave the desired substituted guanidino tertiary amides series **IA** and **IB** (**15a–15g** and **16a–16g**) in good yields (Scheme 3). Additionally, to design the third series of substituted guanidino tertiary amides, the amino tertiary amides (**12a** and **12b**) and compounds **11a–11i** in DMF were treated with anhydrous triethylamine Et₃N before the addition of mercuric chloride in small portions at 0 °C to produce the Boc-protected guanidino tertiary amides **17a–17i** and **18a–18i** (Scheme 4). After that, Boc groups were eliminated using TFA in DCM to form the second series **A** and **B** (**19a–19d** and **20a–20c**) and the third series **A** and **B** (**19e–19i** and **20e–20i**) of substituted guanidino tertiary amides in moderate yield (Scheme 4). The procedures of synthesis and characterization data of the lipophilic and cationic tertiary amides are available in the experimental section of the SI S1–S70.

Antibacterial activity

The antibacterial activities of the substituted guanidino lipophilic and cationic tertiary amides were evaluated against six bacterial strains: Gram-positive bacteria *S. aureus* (SA38, ATCC 6538, ATCC 25923); and Gram-negative bacteria (*E. coli* K12, *E. coli* ATCC 25922), and *P. aeruginosa* (PA01). The activity of the substituted guanidino tertiary amides was compared with the activity of MSI-78 (Pexiganan, an AMP). The MIC and toxicity values are reported in Table 1 (see the experiment protocol in the SI).
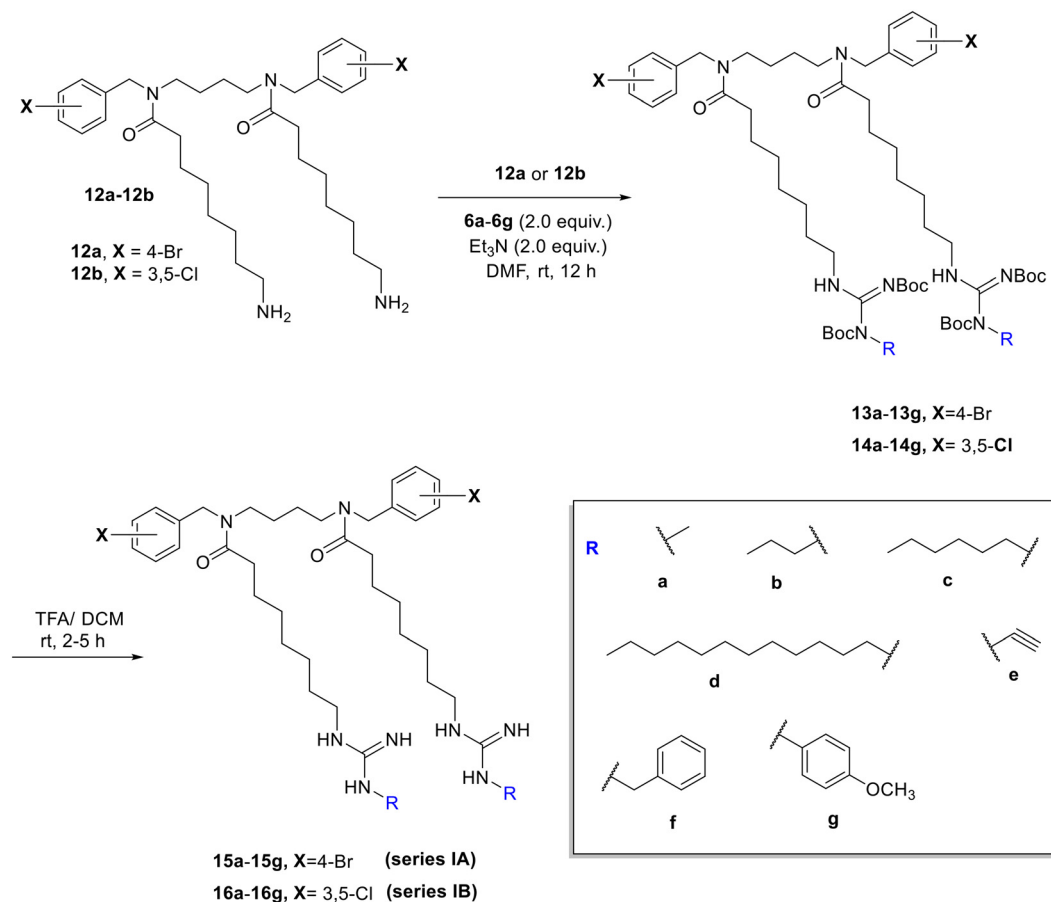
In general, the majority of the synthesized tertiary amides had excellent activity against *S. aureus* strains with MICs ranging from 1 µg mL⁻¹ to 8 µg mL⁻¹. Additionally, compared

to the previously synthesized tertiary amides,[32,33] where only two compounds had excellent activity against *E. coli* strains with MIC of 6.2 µg mL⁻¹, in this work, a range of active tertiary amides had excellent activity against Gram-negative bacteria, especially *E. coli*, with an average MIC of 4–8 µg mL⁻¹.

In the first series with **IA** (bromo derivatives) and **IB** (chloro derivatives) of alkyl-substituted guanidino tertiary amides **15a–15d** and **16a–16d**, the antibacterial activity against *S. aureus* and *E. coli* K12 decreased as the length of the alkyl chain increased. The guanidino methyl, propyl, and propyne tertiary amides (**15a, 15b, 15e, 16a, 16b,** and **16e**) were the most active lipo-tertiary amides against *S. aureus* with MICs around 1.6 µg mL⁻¹, while hexyl derivatives **15c** and **16c** showed a slight reduction in the activity by two-fold and four-fold against *S. aureus* with MICs of 3.7 and 7.3 µg mL⁻¹ respectively. The attachment of the dodecyl lipid chain (12C) to the guanidine part in compounds **15d** and **16d** caused a loss of antibacterial activity against *S. aureus*.

The alteration in activity resulting from the insertion of an aromatic (phenyl and 4-methoxyphenyl) hydrophobic group instead of an alkyl tail was investigated in compounds **15f–15g** and **16f–16g**. The bromo tertiary amide **15f** was slightly more active against *S. aureus* than chloro tertiary amide **16f** with MICs of 3.8 and 7.4 µg mL⁻¹, respectively. The insertion of the methoxy group (OCH₃) on the guanidino phenyl ring in compounds **15g** and **16g** reduced their activity, with MICs around 16 µg mL⁻¹. In the same series (**IA** and **IB**), as with the activity against *S. aureus*, the activity against *E. coli* was reduced by increasing the alkyl chain. The methylated guanidino compounds **15a** and **16a** showed

Scheme 3 The preparation of the first series of substituted guanidine lipophilic tertiary amides using substituted carboxamidine reagents (**6a–6g**).

activity with MICs of 6.2 μg mL^{-1}, while this activity was decreased for propyl and propyne guanidino compounds **15b**, **16b** and **16e** with MICs of approximately 13.5 μg mL^{-1} and **15e** with MIC of up to 27 μg mL^{-1}. The activity continued to decrease by increasing the alkyl tail length; the hexyl guanidino bromo tertiary amide **15c** had MIC of 60 μg mL^{-1}, whereas the hexyl guanidino chloro tertiary amide **16c** and dodecyl guanidino tertiary amides (**15d** and **16d**) were inactive against *E. coli* K12.

The bromo tertiary amides **15f** and **15g** (with phenyl and 4-methoxy phenyl attached to the guanidino group) showed moderate activity against *E. coli* with MICs around 15.5 μg mL^{-1}, whereas the dichloro tertiary amides **16f** and **16g** (with phenyl and 4-methoxy phenyl attached to the guanidine group) were inactive against *E. coli* K12.

A log *P* values represent the lipophilicity of the guanidino lipo-tertiary amides (**15** and **16**). The activity decreased with an increase in the lipophilicity of the molecule (A log *P* values). This is clear from the low A log *P* values of the most active methylated guanidino compounds **15a** and **16a** (A log *P* = 6.9 and 7.8) compared to the high A log *P* values of dodecyl guanidino tertiary amides **15d** and **16d** (A log *P* = 16.7 and 17.5).

Additionally, all the designed lipo-tertiary amides of series **IA** and **IB** were inactive (MIC ≥ 200 μg mL^{-1}) against PA01.

Fig. 3A summarizes the activity of these lipophilic tertiary amides against *S. aureus* 38 and *E. coli* K12.
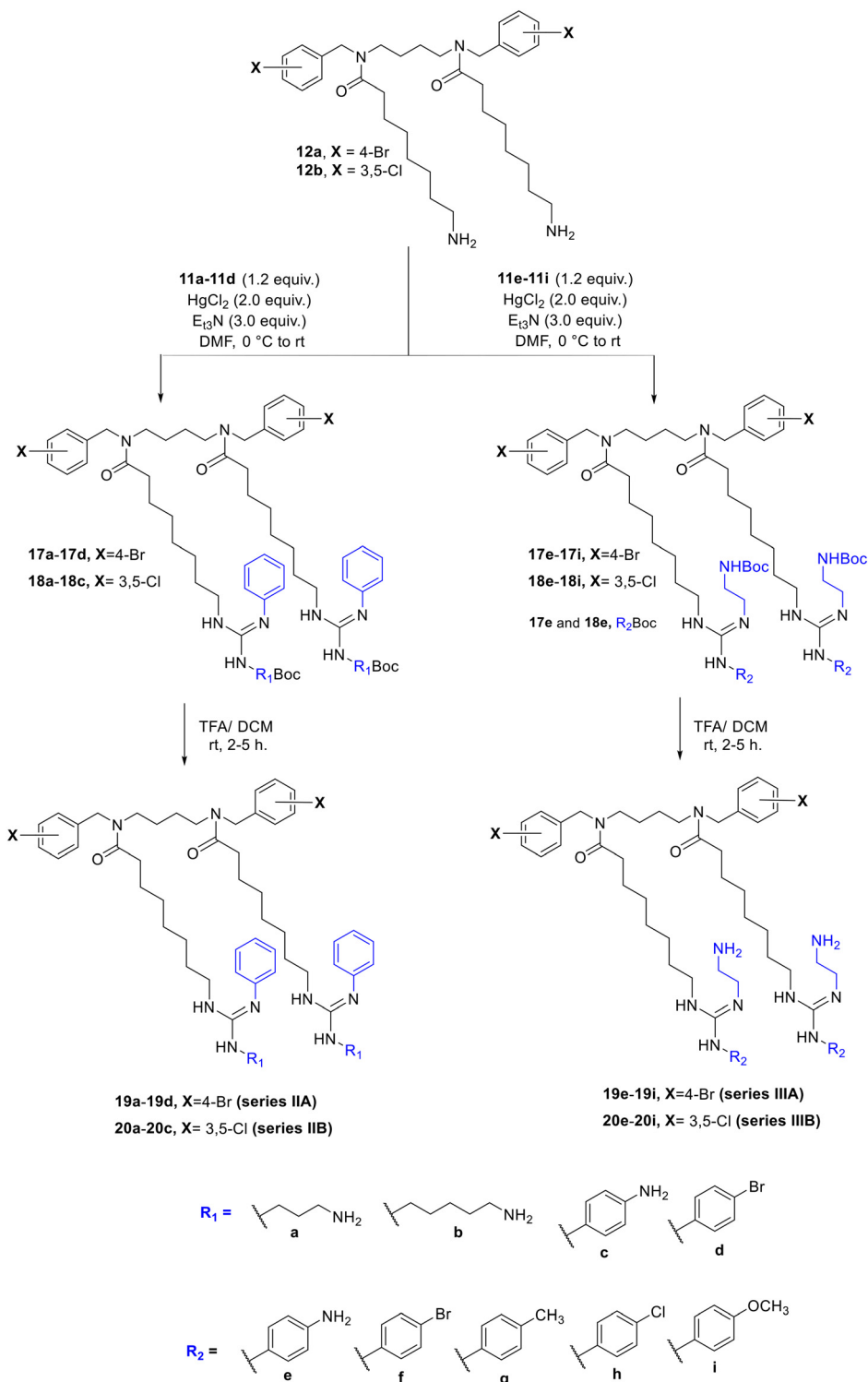
In the second series **II**, two groups were attached to the guanidine to form series **IIA** (**19a–19d**) and series **IIB** (**20a–20d**); one side of the guanidine groups has a cationic group, and the other side a phenyl group.

The activities of the bromophenyl substituted-guanidino tertiary amides series **IIA** (**19a–19d**) and dichlorophenyl substituted-guanidino tertiary amides series **IIB** (**20a–20c**) were evaluated against all the bacterial strains. Compound **19d** was an interesting compound that lost antimicrobial activity when the cationic side was replaced with an additional hydrophobic group.

The compounds **19a**, **19b**, **20a**, and **20b** of series **IIA** and **IIB** were the most active molecules against the bacterial strains among all the designed lipophilic and cationic tertiary amides with MICs of 1–2 μg mL^{-1} against *S. aureus*, 2.3–3.9 μg mL^{-1} against *E. coli* and 16.5–35.5 μg mL^{-1} against *P. aeruginosa* PA01. Compound **19a** was the most active compound against *P. aeruginosa* PA01 with MIC of 16.5 μg mL^{-1}.

The best activities of these compounds, **19a–b** and **20a–b**, could be attributed to the free cationic group that was attached by the 3C and 6C alkyl chains to the bottom side of the guanidine group. The change of the alkyl linker from 3C

Scheme 4 The preparation of the second and third series of substituted guanidine cationic tertiary amides using substituted thiourea reagents (**11a–11i**).

(**19a** and **20a**) to 6C (**19b** and **20b**) did not change the activity. In the case of compounds **19c** and **20c**, the attachment of an aryl cationic group (aniline) decreased the activity against *S. aureus* with MIC around 17.5 μg mL^{-1} compared to 1–2 μg mL^{-1} for **19a–b** and **20a–b**. Moreover, compounds **19c** and

20c lost the activity against Gram-negative bacteria compared to the active compounds **19a–b** and **20a–b**. The replacement of the cationic group NH$_2$ on **19c** with Br produced compound **19d**. This replacement reduced the cationicity and increased the hydrophobicity of **19d**, with a high Alog*P* value

Table 1 Antibacterial activity (MICs), and hemolytic activity (HC) of lipophilic and cationic tertiary amides[a]

| ID | Series | MIC (μg mL^{-1}) | | | | | | HC (μg mL^{-1}) | | |
		S. aureus 38	S. aureus ATCC 6538	S. aureus ATCC 25923	E. coli K12	E. coli ATCC 25922	PA01	HC$_{10}$	HC$_{50}$	Alog P
15a	**IA**	**1.6**	**1.6**	**1.6**	6.2	6.2	>205	>9.8	20.5	6.87
15b		**1.7**	**1.7**	**1.7**	13.8	13.8	219	10.5	21.9	8.63
15c		3.7	3.7	7.5	60	60	>240	24	48	11.30
15d		>282	NT	NT	>282	NT	NT	112.9	451.7	16.63
15e		**1.7**	**1.7**	**1.7**	27	13.5	217	17.4	>21.5	7.33
15f		3.8	3.8	3.8	15.2	15.2	243	24.3	>48.6	10.32
15g		16	NT	16	16	16	NT	25.8	>51.6	10.01
16a	**IB**	**1.6**	**1.6**	**1.6**	6.2	6.2	200	9.6	16	7.75
16b		**1.7**	**1.7**	**1.7**	13.4	13.4	214	10.3	17.1	9.51
16c		7.3	7.3	7.3	>235	NT	NT	18.8	23.5	12.18
16d		>277	NT	NT	>277	NT	NT	110.9	>444	17.51
16e		**1.7**	**1.7**	**1.7**	13.2	6.6	216	16.9	16.9	8.21
16f		7.4	7.4	7.4	119	NT	NT	>23.8	>47.6	11.20
16g		15.8	15.8	15.8	>253	NT	NT	6.1	12.2	10.89
19a	**IIA**	**1**	**1**	**1**	**4.1**	**2**	**16.5**	26.5	>52.9	9.03
19b		**2.2**	**2.2**	**1.1**	**4.4**	**2.2**	35.6	28.6	57.2	11.84
19c		17.6	17.6	17.6	>282	NT	>282	13.5	28.2	12.66
19d		>313	NT	NT	>313	NT	>313	125.5	>502	15.86
20a	**IIB**	**2**	**2**	**2**	**4**	**4**	**32.4**	12.5	20.8	9.91
20b		**1.1**	**1.1**	**1.1**	**4.4**	**4.4**	35.6	13.5	22.5	12.72
20c		17.3	17.3	17.3	>277	NT	>277	27.8	55.4	13.54
19e	**IIIA**	8.3	8.3	8.3	8.3	8.3	**33**	53.1	>106	7.88
19f		4.6	9.3	9.3	9.3	18.5	74.2	>59.4	>119	11.08
19g		**2.1**	**2.1**	**4.1**	**4.1**	**4.1**	66.1	21.2	26.5	10.57
19h		4.3	4.3	4.3	17.3	17.3	68.6	>54.9	>110	10.75
19i		**2.1**	**2.1**	**2.1**	**4.2**	**2.1**	**34**	21.8	27.3	9.22
20e	**IIIB**	8.1	8.1	8.1	8.1	8.1	**32.5**	26.0	>52.1	8.76
20f		4.5	9.1	9.1	72.9	146	292.2	>58.4	>117	11.96
20g		4	4	4	8.1	16.2	64.8	12.5	20.7	11.45
20i		**2.1**	**2.1**	**2.1**	**4.2**	**4.2**	66.8	12.9	21.4	10.10
MSI-78 (ref. 34–38)		1.3–2.6	—	4.0	1.3–2.6	8.0–16.0	1.3–2.6	—	—	4.52

[a] NT (not tested); PA01 (*P. aeruginosa* strain PA01); bolded MICs represent the most active molecules against *S. aureus* (MIC < 2.5 μg mL^{-1}), *E. coli* (MIC < 5 μg mL^{-1}), and PA01 (MIC < 36 μg mL^{-1}); HC = hemolytic concentration giving 10% or 50% hemolysis; Alog P is a measure of lipophilicity/hydrophobicity.

of 15.9, which resulted in the loss of activity against all bacterial strains, highlighting the importance of maintaining a balance between the cationic and hydrophobic components in these tertiary amides. Fig. 3B shows a comparison between the MIC values of series **II** derivatives against *S. aureus* 38 and *E. coli* K12.

In series **III** compounds **19e–19i** and **20e–20i**, the cationic group (ethylamine group) was linked to the sides of the guanidine groups, and the bottom side was attached to different 4-substituted phenyl rings (4-(bromo, methyl, chloro, or methoxy)-phenyl). As shown in Fig. 3C and Table 1, the compounds **19f–19i** and **20f–20i** showed the same range of activity against *S. aureus* with MICs of 2.1–4.6 μg mL^{-1}, which indicates that the activity is attributed to the cationic group regardless of the type of hydrophobic group. Also, the lipophilicity did not play a role in the activity of compounds **19f–19i** and **20f–20i**, which is evident from the very similar Alog P values of these tertiary amides (Table 1). Compounds that had methyl or methoxy groups (**19g**, **19i**, **20g**, and **20i**) showed more activity against *E. coli* strains with 4.1, 4.2, 8.1,

and 4.2 μg mL^{-1}, respectively, compared to **19f**, **19h**, and **20f** (which contain additional chlorine and bromine atoms) with MIC of 9.3, 17.3, and 72.9 μg mL^{-1}, respectively (Table 1 and Fig. 3C).

Compounds **19e** and **20e** have two cationic sides, with an additional one (NH$_2$) which is attached to the *para* position of the phenyl ring. These two compounds, **19e** and **20e**, exhibited equal activity against *S. aureus* and *E. coli*, with MICs of approximately 8 μg mL^{-1}. The best active compounds in series **III** against PA01 were **19e**, **20e** (aniline derivatives), and **19i**, with MICs ranging from 32.5 μg mL^{-1} to 34 μg mL^{-1}. In contrast, other compounds in the same groups showed less activity, with MICs of 64.8–74.2 μg mL^{-1}, except for **20f**, which was inactive against PA01. Furthermore, the activity of the active compounds in series **I**, **II**, and **III** was evaluated against other Gram-positive and Gram-negative bacterial strains, and their activity was similar to that against *S. aureus* 38 and *E. coli* K12.

The structure–activity relationship (SAR) of bromophenyl-substituted guanidine and dichlorophenyl-substituted guanidine
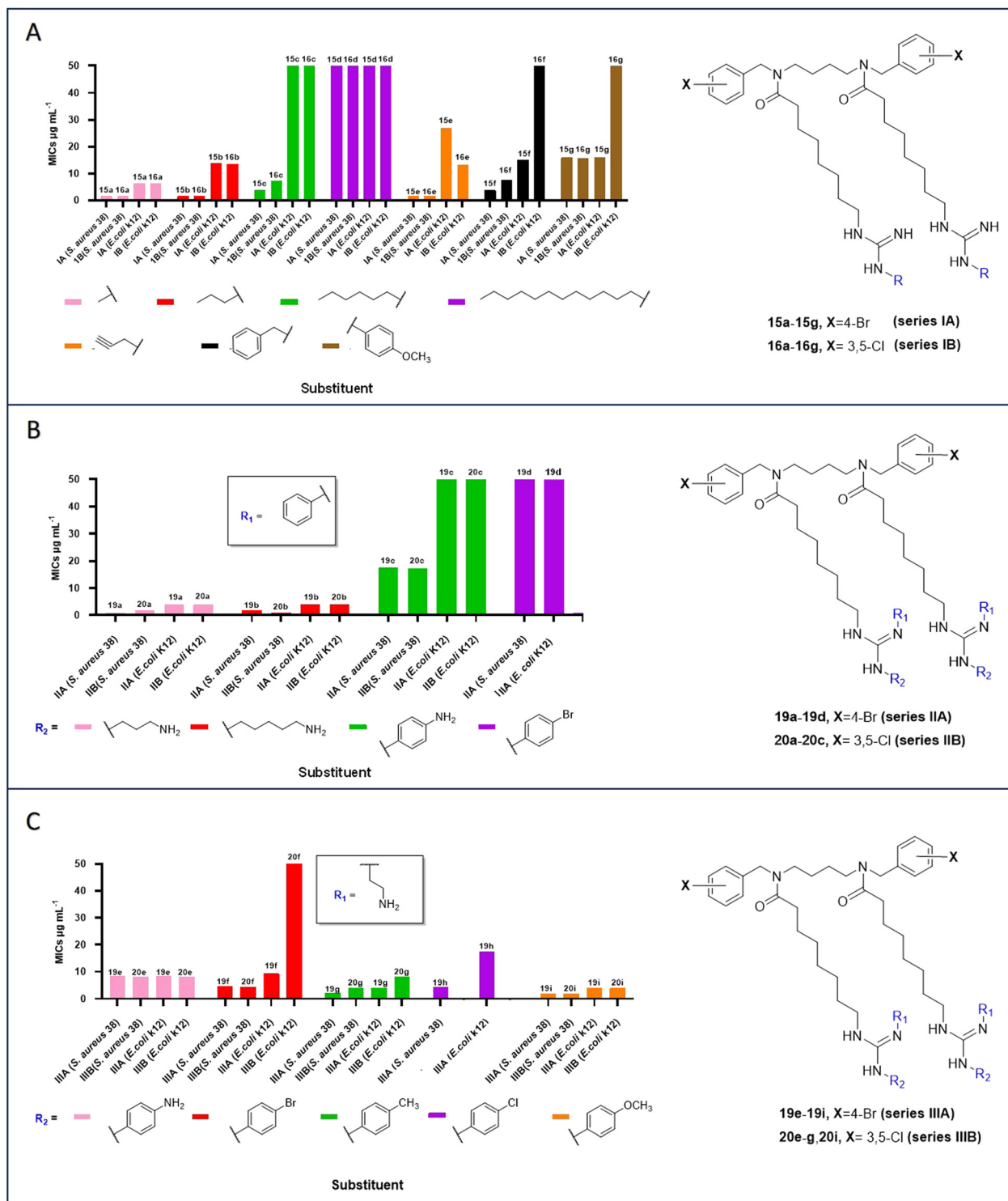
Fig. 3 The antibacterial activity of series I (A), II (B), and III (C) against *S. aureus* 38 and *E. coli* K12 as represented by the MIC values.

tertiary amides. The activity was evaluated based on the attachment of lipophilic (series **I**) or cationic and hydrophobic (series **II** and **III**) groups on the guanidine that attached to a rigid amide structure. In series **I**, the dimeric compounds with the shorter alkyl group attached to guanidine (**15a–b** and **16a–b**) were the most active, while those with the longest alkyl groups (**15d** and **16d**) were inactive. The addition of phenyl and methoxyphenyl groups instead of the alkyl resulted in compounds with less activity compared with short lipidic compounds. Interestingly, these activities increased with the reduction in lipophilicity, as indicated by the A log *P* values in Table 1.

Series **II** contains the most active structures **19a–b** and **20a–b** that include guanidine groups bearing a phenyl ring and cationic alkyl tails. In this series, when the cationic alkyl chain of **19a–b** and **20a–b** was replaced by an aryl cationic group (aniline) (**19c** and **20c**), the activity decreased due to the increase in lipophilicity. Additionally, the replacement of the NH$_2$ group on the aniline moiety by a bromine atom (**19d**) resulted in complete loss of antibacterial activity (with the highest Alog$P$ value of 15.8).

In series **III**, all peptoids had a good activity (the MIC values in this group were slightly similar or very close), especially against Gram-positive bacteria, because all these compounds contain the same cationic group (ethylamine group) on one side of the guanidine, and the other side contained a substituted phenyl group. The lipophilicity did not play a clear role in the activity of this series of tertiary amides. Methyl and methoxy-phenyl derivatives of this series were the most active derivatives against *S. aureus* and *E. coli*, while aniline analogs were the most active derivatives against PA01. The SAR of the substituted guanidine tertiary amides is outlined in Fig. 4.

Fisher Scientific, HB250) and is represented as their HC$_{10}$ (concentration producing a maximum 10% hemolysis) and HC$_{50}$ (concentration producing a maximum 50% hemolysis) values (Table 1). In general, all bromo tertiary amides of series **IA**, **IIA**, and **IIIA** showed lower toxicity against mammalian blood cells and higher therapeutic doses compared to chloro tertiary amides series **IB**, **IIB**, and **IIIB**. Additionally, the most active cationic substituted guanidino tertiary amides **19a** and **19b** of series **II** exhibited lower levels of hemolysis (1–5%) at 25 μg mL^{-1} compared to the active lipophilic guanidino tertiary amides **15a–b**, **16a–b** of series **I**. The most active compounds against all tested bacterial strains with the lowest toxicity were compounds **19a** and **19b**, which had MICs of 1–2 μg mL^{-1} against *S. aureus* 38 and therapeutic indices (TI) of 52.9 and 24.9 times of their MICs, respectively. Also, they had therapeutic indices (TIs) of 13 times their MICs against *E. coli*, and TIs of 3.2 and 1.6 against PA01, respectively (TI = HC/MIC). Table 2 shows the therapeutic index (TI) and selectivity ratio (SR) of the active tertiary amides against *S. aureus* 38, *E. coli* K12, and PA01 (see the experiment protocol in the SI).

Hemolytic activity assay

The toxicity of all substituted guanidino tertiary amides was assessed by their ability to lyse horse red blood cells (Thermo

Antibiofilm activity

The bacterial biofilm has developed various mechanisms to resist the activity of traditional antibiotics and antimicrobial
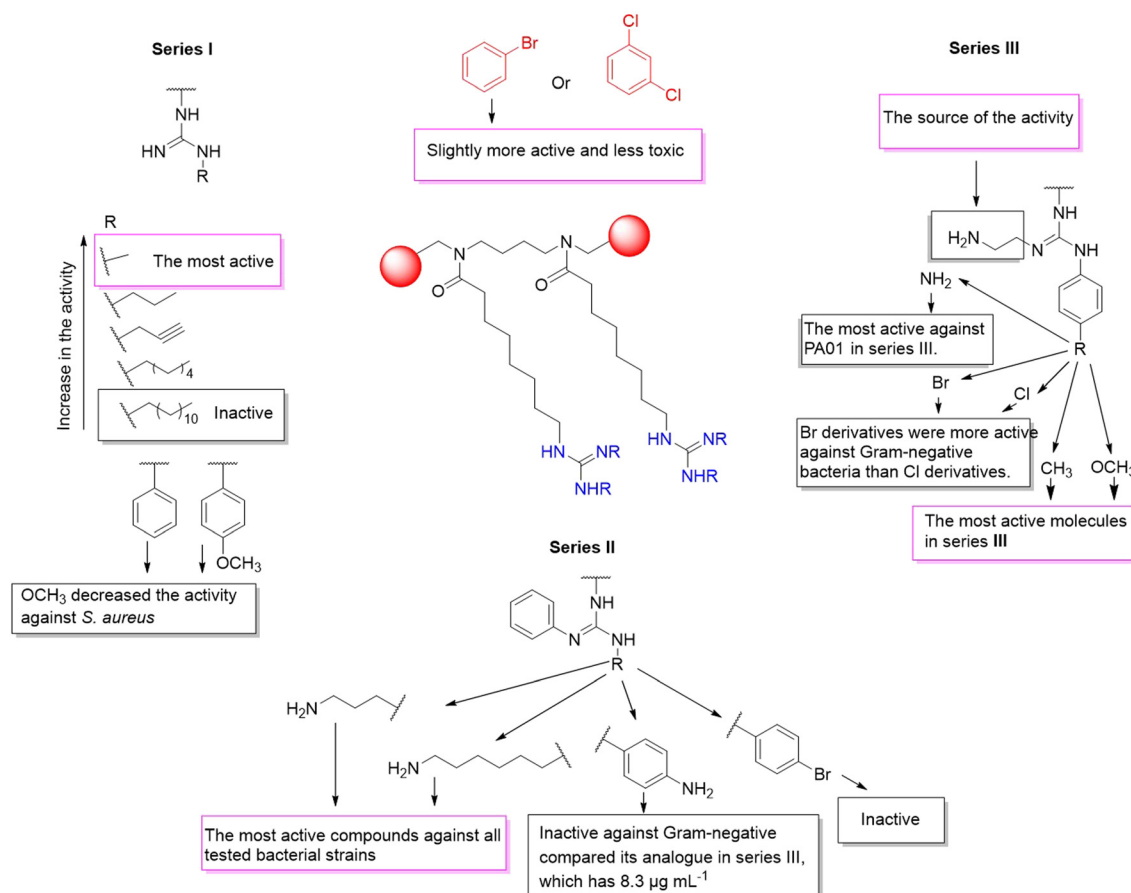

Fig. 4 The structure–activity relationship (SAR) of substituted guanidine bromo and dichloro-phenyl based tertiary amides.

Table 2 Therapeutic index (TI) and selectivity ratio (SR) of the active tertiary amides against *S. aureus* 38, *E. coli* K12, and PA01[a]

ID	HD/HC (μg mL^{-1})		MIC (μg mL^{-1})			Therapeutic index (TI)			Selectivity ratio (SR)		
	HD$_{10}$/HC$_{10}$	HD$_{50}$/HC$_{10}$	*S. aureus* 38	*E. coli* K12	PA01	TI$_S$	TI$_E$	TI$_P$	SR$_S$	SR$_E$	SR$_P$
15a	9.8	20.5	1.6	6.2	205	12.8	3.3	0.1	6.1	1.6	0.1
15b	10.5	21.9	1.7	13.8	219	12.8	1.6	0.1	6.2	0.7	0.1
15c	24	48	3.7	60	240	12.9	0.8	0.2	6.5	0.4	0.1
15e	17.4	21.5	1.7	27	217	12.6	0.8	0.1	10.2	0.6	0.1
15f	24.3	48.6	3.8	15.2	243	12.7	3.2	0.2	6.4	1.6	0.1
16a	9.6	16	1.6	6.2	200	10	2.6	0.1	6	1.5	0.1
16b	10.3	17.1	1.7	13.4	214	10.1	1.3	0.1	6.1	0.7	0.1
16e	16.9	16.9	1.7	13.2	216	9.9	1.3	0.1	9.9	1.3	0.1
19a	26.5	52.9	1	4.1	16.5	52.9	12.9	3.2	26.5	6.4	1.6
19b	28.6	57.2	2.3	4.4	35.6	24.8	13	1.6	12.4	6.5	0.8
20a	12.5	20.8	2	4	32.4	10.4	5.2	0.6	6.2	3.1	0.4
20b	13.5	22.5	1.1	4.4	35.6	20.4	5.1	0.6	12.3	3.1	0.4
19e	53.1	106	8.3	8.3	33	12.7	12.7	3.2	6.4	6.4	1.6
19f	59.4	119	4.6	9.3	74.2	25.8	12.8	1.6	12.9	6.4	0.8
19g	21.2	26.5	2.1	4.1	66.1	12.6	6.5	0.4	10.1	5.2	0.3
19h	54.9	110	4.3	17.3	68.6	25.6	6.4	1.6	12.7	3.2	0.8
19i	21.8	27.3	2.1	4.2	34	13	6.5	0.8	10.4	5.2	0.6
20f	58.4	117	4.5	72.9	292.2	26	1.6	0.4	12.9	0.8	0.2
20g	12.5	20.7	4	8.1	64.8	5.2	2.5	0.3	3.1	1.5	0.2
20i	12.9	21.4	2.1	4.2	66.8	10.2	5.1	0.3	6.1	3.1	0.2

[a] HD$_{10}$ (10% haemolytic dose), HD$_{50}$ (50% haemolytic dose), TI = HD$_{50}$/MIC, SR = HD$_{10}$/MIC. TI$_S$, TI$_E$, TI$_P$, SR$_S$, SR$_E$, and SR$_P$ (therapeutic indices and the selectivity ratios against *S. aureus* 38, *E. coli* K12, and PA01, respectively).

agents, which has made the treatment of biofilm-associated acute infections a critical issue in this era.[39–41] Conventional antibiotics and antimicrobials are inactive against infections caused by bacteria in their biofilm state.[41] Therefore, the antibiofilm activity of the active tertiary amides was investigated against pre-established biofilms of Gram-positive (*S. aureus* 38) and Gram-negative bacteria (*E. coli* K12).

The active tertiary amides with additional cationic groups **19a**, **20a**, **19b**, **20b**, **19e**, **19g**, **19i**, and **20i** were selected to measure their ability to disrupt the pre-established biofilms of *S. aureus* 38 using the crystal violet (CV) staining assay (Fig. 5A–C). All the compounds were tested at three concentrations: 2×, 4×, and 8× MIC. At all concentrations of 2×, 4×, and 8× MIC, the best disruptor of *S. aureus* 38 pre-established biofilms was aminohexyl guanidinium bromo-tertiary amides **19b** with 42%, 51%, and 75% disruption of the biofilm, respectively. This activity could be a result of the free long tail (hexyl) that holds the cationic group. Additionally, at 2× MIC, the short version of compound **19b** (compound **19a**), featuring an amino-propyl tail, was the second with 18% disruption of *S. aureus* 38 biofilms. The remaining compounds, **20a**, **20b**, **19e**, **19g**, **19i**, and **20i**, at 2× MIC eradicated less than 10% of the biofilms of *S. aureus* 38. At 4× MIC, aniline guanidino bromo-tertiary amide **19e** was the best biofilm disruptor after **19b**, with 42% reduction in the *S. aureus* 38 biomass (Fig. 5A). At 4× MIC, the remaining compounds **19a**, **20a**, **20b**, **19g**, **19i**, and **20i** disrupted 37%, 27%, 28%, 18%, 22%, and 38% of the *S. aureus* 38 biomass, respectively (Fig. 5B). Compound **20b** (aminohexyl guanidinium chloro-tertiary amide) showed a considerable reduction of the *S. aureus* 38 biofilms with 55% reduction at 8× MIC compared to 9% at 2× MIC and compound **19e**

reduced more of the *S. aureus* 38 biomass (55%). At 8× MIC, the short version of **19b** and **20b**, compounds **19a** and **20a**, disrupted around 50% of the *S. aureus* 38 pre-established biofilms, while the ethylamine guanidino tertiary amides **19g**, **19i**, and **20i** (with methyl and methoxy groups) have the lowest activity against *S. aureus* 38 biofilm with around 35% disruption. Interestingly, the majority of bromo derivatives, especially at low concentrations, disrupt the *S. aureus* 38 biofilms faster than chloro derivatives (Fig. 5C) (see the experiment protocol in the SI).

Moreover, the antibiofilm activity of the same active cationic tertiary amides **19a**, **20a**, **19b**, **20b**, **19e**, **19g**, **19i**, and **20i** was investigated against eradicating established biofilms of *E. coli* K12 (Fig. 5D–F). At 2× MIC, compounds **19b** (amino-hexyl guanidino bromo-phenyl-based tertiary amide) and **20a** (amino-propyl guanidino dichloro-phenyl-based tertiary amide) were the best compounds with approximately 20% disruption of *E. coli* biomass, while compounds **19a** (amino-propyl of bromo-tertiary amide) and **19g** (methylated phenyl of bromo-tertiary amide) came in the second place with 15% disruption. The remaining tertiary amides **20b**, **19e**, **19i**, and **20i** showed less than 10% reduction in the *E. coli* biofilms (Fig. 5D).

At 4× MIC, compounds **19b** and **20a** disrupted 35% of *E. coli* biomass, whereas compounds **19a** and **19g** (aminoethyl and methylated phenyl guanidines) disrupted 30% of it. Additionally, at 4× MIC, the other tested tertiary amides **20b** and **19e** reduced 19% and 15% of the biomass of *E. coli* K12, respectively, while methoxy phenyl guanidino tertiary amides **19i** and **20i** disrupted only 7% of the *E. coli* K12 biofilms (Fig. 5E). At the highest concentration (8× MIC), compound **19g** (with aminoethyl cationic group and methyl phenyl
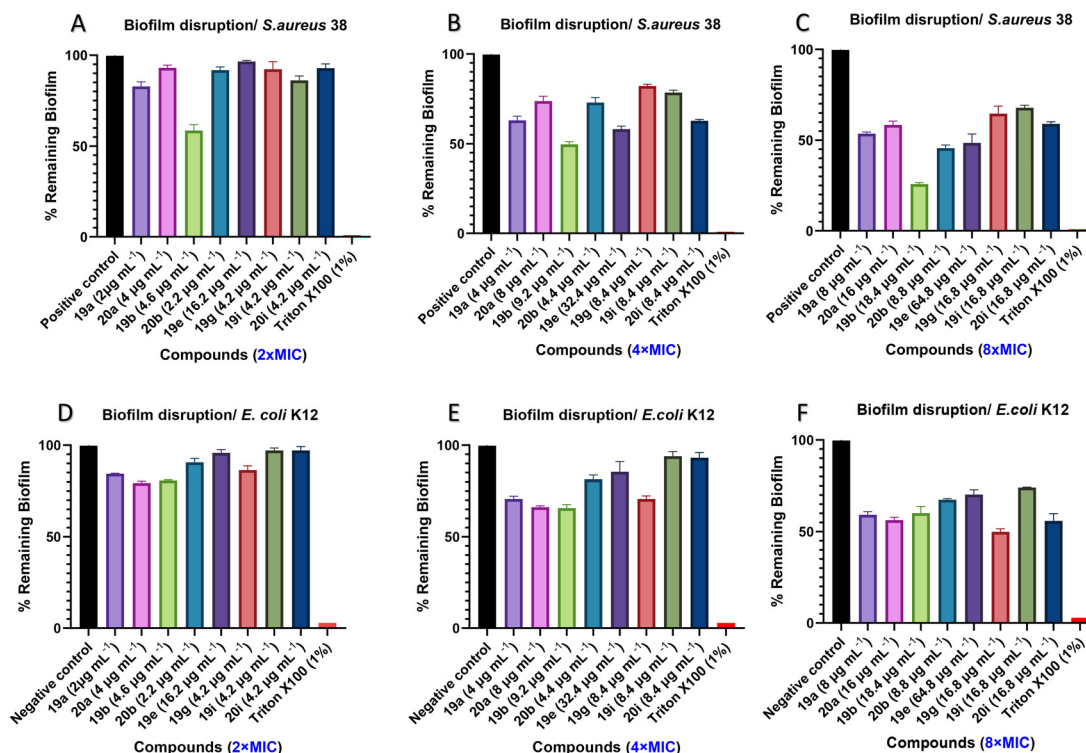
Fig. 5 Disruption of established biofilms of *S. aureus* 38 (A–C) and *E. coli* K12 (D–F) after 24 h treatment with 2×, 4×, and 8× MIC concentrations of compounds **19a**, **20a**, **19b**, **20b**, **19e**, **19g**, **19i**, and **20i**, respectively. The positive control represents pre-established *S. aureus* 38 and *E. coli* K12 biofilms without any compounds. Triton X-100 represents the negative control. Error bars indicate the standard error of three independent experiments.

group connected to the guanidine part) and **20i** (with aminoethyl cationic group and methoxy phenyl group connected to the guanidine part) were the best disruptors, with 50% and 45% disruption of the *E. coli* K12 biofilm, respectively. On the other hand, compounds **19a**, **20a**, and **19b** showed a 40% reduction of the *E. coli* K12 biomass at 8× MIC. The remaining compounds (**20b**, **19e**, and **19i**) disrupted about 30% of the *E. coli* K12 biomass (Fig. 5F).

Cytoplasmic membrane depolarization

To examine the potential disruption effect of tertiary amides on the bacterial cytoplasmic membrane, the diSC3-5 (3,3′-dipropyl-thiadicarbocyanine iodide) as a membrane potential-sensitive dye was used (see the experiment protocol in the SI). The dye directly partitions into the membrane of bacterial cells and aggregates throughout the membrane, causing self-quenching of fluorescence. If the substituted guanidino tertiary amide has the ability to disrupt the bacterial cytoplasmic membrane, the dye will be released because of the bacterial cell membrane depolarizes or is damaged. An increase in fluorescence will be observed due to the increased flow of the dye out of the damaged bacterial membranes. Compounds **19a** and **19b**, which had the best activity against both Gram-positive and Gram-negative strains and the lowest toxicity, were selected to study their ability to damage the bacterial cytoplasmic membrane.

The two compounds **19a** and **19b** were added at 0.5×, 1×, 2×, and 4× MIC, which caused damage to the cell membranes of *S. aureus* 38 and *E. coli* K12 in a time and concentration-dependent manner (Fig. 6). In general, at 4× MIC levels, both compounds **19a** and **19b** affected the *S. aureus* 38 and *E. coli* K12 membranes within 3 minutes with an increase in the fluorescence. At the lowest concentration of 0.5× and 0.1× MIC, compound **19a** (aminopropyl guanidino tertiary amide) affected the cell membrane within 3 min (Fig. 6A), while **19b** (aminohexyl guanidino tertiary amide) did not cause any changes in the fluorescence at the lowest concentrations (0.5× and 0.1× MIC) (Fig. 6B). The fast effect of compound **19a** on the bacterial cell membrane at 0.5× MIC compared to **19b** could be due to the effect of the low lipophilicity (Alog P = 9) of the shorter side chain length of the cationic tail of compound **19a** compared to that of compound **19b** (Alog P = 12). As shown in Fig. 6A, compound **19a** increased the fluorescence gradually and in a steady line at 0.5×, 1× and 2× until it reached the peak at 4× MIC within 12–15 minutes due to its effect on the *S. aureus* 38 cytoplasmic membrane. The addition of compound **19b** at 2× and 4× MIC on the *S. aureus* 38 cytoplasmic membrane caused an increase in fluorescence level before reaching the peak of fluorescence at 4× MIC within 9 minutes up to 15 minutes (Fig. 6B). Similar to the effect of **19a** on the *S. aureus* 38 membrane, compound **19a** affected the *E. coli* K12 membrane at 0.5× MIC, maintaining a constant fluorescence level from 3 minutes to 15 minutes. In contrast, at 1×, 2×, and 4× MIC, the fluorescence increased slightly over time (Fig. 6E).
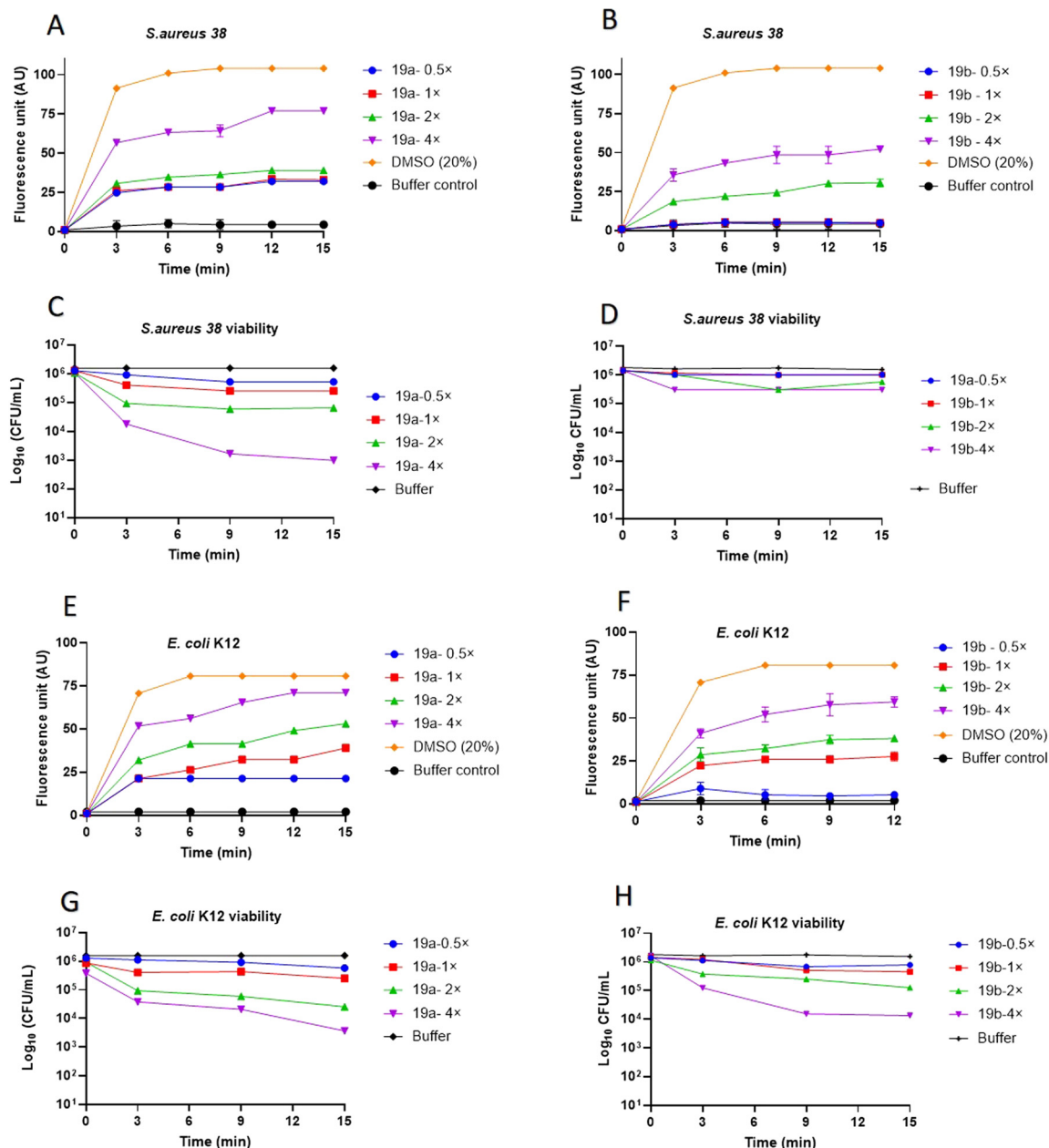
Fig. 6 *S. aureus* 38 cytoplasmic membrane disruption that was promoted at different concentrations (A and B) by **19a** (0.5 µg mL^{-1}, 1 µg mL^{-1}, 2 µg mL^{-1}, 4 µg mL^{-1}) and **19b** (1 µg mL^{-1}, 2.3 µg mL^{-1}, 4.6 µg mL^{-1}, 8.6 µg mL^{-1}). *E. coli* K12 cytoplasmic membrane disruption that was promoted at different concentrations (E and F) by **19a** (2 µg mL^{-1}, 4.1 µg mL^{-1}, 8.2 µg mL^{-1}, 16.4 µg mL^{-1}) and **19b** (2.2 µg mL^{-1}, 4.4 µg mL^{-1}, 8.8 µg mL^{-1}, 17.6 µg mL^{-1}). 20% DMSO was used as a positive control. C, D, G, and H represent *S. aureus* 38 and *E. coli* K12 cell viability count in the presence of **19a** and **19b** at the same concentrations that were used for cytoplasmic membrane disruption.

In the case of the impact of compound **19b** on the *E. coli* K12 at 0.5× MIC, there was no noticeable change in the fluorescence, whilst at 1× and 2× MIC, the fluorescence was increased slightly by increasing the time before reaching the maximum release of the dye at its 4× MIC (Fig. 6F). Moreover, to investigate the responsible mechanism for cell killing, the effects of cationic tertiary amides **19a** and **19b** on the viability of *S. aureus* 38 and *E. coli* K-12 cells have been analysed (Fig. 6C, D, G, and H). In general, the cell viability of compounds **19a** and **19b** against *S. aureus* 38 and *E. coli* K12

resembled the results observed in membrane disruption experiments. At 4× MIC, compound **19a** showed almost 3 log reductions in *S. aureus* 38 bacterial numbers within 9 min, and these results coincide with the results of the dye release assay as well, while compound **19b** showed more than 5 log reductions in *S. aureus* 38 bacterial numbers within 15 min (Fig. 6C and D). In the case of *E. coli* K12 bacterial numbers, compound **19a** and **19b** caused about a 4 log decrease in the bacterial numbers within 9 minutes, followed by a reduction of 3 log at 15 minutes for the aminohexyl tertiary amide **19b**

(Fig. 6G and H). Depending on these results, membrane permeabilization could be a possible mechanism for the substituted guanidino tertiary amides effects over a short time, but there may be longer-term effects that lead to bacterial cell killing. These influences might involve the release of autolysins, similar to the antimicrobial peptides melimine and Mel4.

Quartz Crystal Microbalance with Dissipation (QCM-D)

The mode of action of the most active tertiary amides, **19a** and **19b** (Fig. 7), was also studied using a nanogram-sensitive technique, Quartz Crystal Microbalance with Dissipation (QCM-D) (see the experiment protocol in the SI). The QCM-D method investigates the response of the antibacterial peptides towards lipid membranes.[42] The QCM-D analysis shows the changes in two parameters over five harmonics or overtones (3rd, 5th, 7th, 9th, and 11th). Frequency (F) represents the mass of the membrane and additionally deposited compounds, and the change in frequency (ΔF) is proportional to mass changes. Dissipation (D) measures the viscoelasticity of the membrane and the change in dissipation (ΔD) provides insight into structural alterations by the addition of tertiary amides. In both cases, the impact on different harmonics signifies the effect of the substituted guanidino tertiary amides at different distances to the surface and interaction locations can thus be determined.[42,43]

In this study, two models of membranes were employed: 100% POPC (a zwitterionic phosphatidylcholine membrane, as found in eukaryotic cells) and 70% POPC with 30% POPG (anionic phosphatidylglycerols mimicking bacterial cell membranes). During the experiment, the compounds (**19a** and **19b**) were added at consecutively increasing concentrations of 5 μM, 10 μM, 20 μM, and 50 μM on the same membrane, incubated for 10 min each then membranes were washed with buffer for 20 min before the next concentration was added.

Interestingly, as shown in Fig. 8A, B and 10A (ΔF–t and ΔD–t plots), compound **19a** (tertiary amides with modified guanidine that bears a propyl amine cationic tail) disrupted the negatively charged model membrane (70% POPC and 30% POPG) at 5 μM with a high positive change of frequency ($+\Delta F$) and negative change of dissipation ($-\Delta D$), while its analogue compound **19b** (including hexyl amine as a cationic group) had a negative frequency change ($-\Delta F$) which increased with increasing concentration, reaching the peak at 50 μM with a small positive change of dissipation ($+\Delta D$) (Fig. 10A) across the concentrations. These differences in response between **19a** and **19b** to their addition to a negatively charged model membrane suggested a different mode or speed in the interaction with the bacterial membrane. This resembled the results from cytoplasmic depolarization studies, as shown in Fig. 6 where compound **19a** is causing the release of the dye at lower concentration compared to **19b** with higher reduction in the live bacteria number. The addition of compound **19a** (5 μM) to the 70% DOPC and 30% POPG lipid layer was sufficient to disrupt the lipidic membrane, as shown in Fig. 8A and B. The addition of compound **19a** (5 μM) led to a considerable decrease in the mass of the membrane affecting the overtone on the membrane surface (3rd) with +5.6 Hz, and slightly less for the inner overtones from +4.9 Hz (5th) to 4.1 Hz (11th), suggesting that the effect is strongest at the membrane surface. Additionally, the positive and high change of ΔF is combined with a decrease of viscoelasticity (increase of rigidity) signified by a negative change of dissipation ($-\Delta D$) (Fig. 8B). Results showing positive ΔF values, negative ΔD values, and the spread of overtones suggested that compound **19a** is disrupting the negatively charged lipidic membrane using the carpet or detergent-like mode of action.[42] This reduction in mass by the addition of 5 μM of **19a** was irreversible after washing (Fig. 8A), whereas rigidity is slightly reversible (Fig. 8B). Additionally, the dynamic effect of compound **19a** in the interaction process on the 70% DOPC
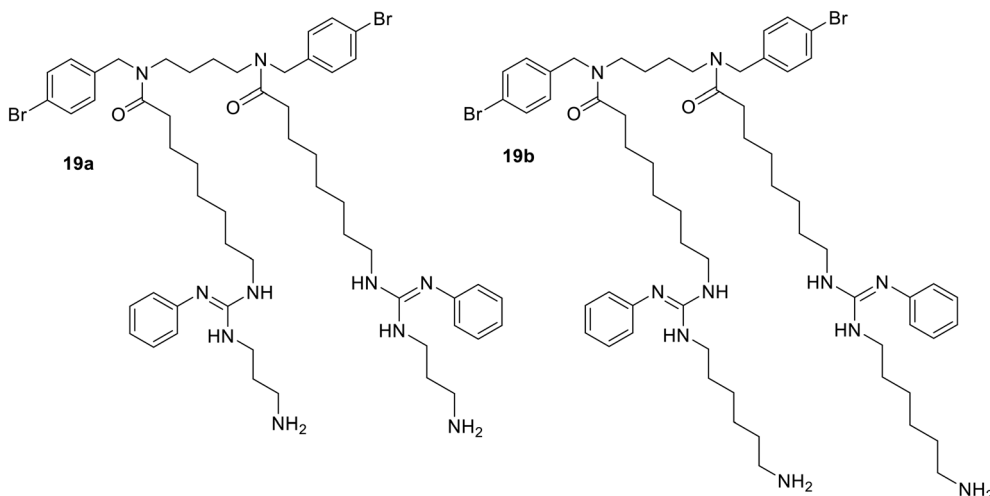

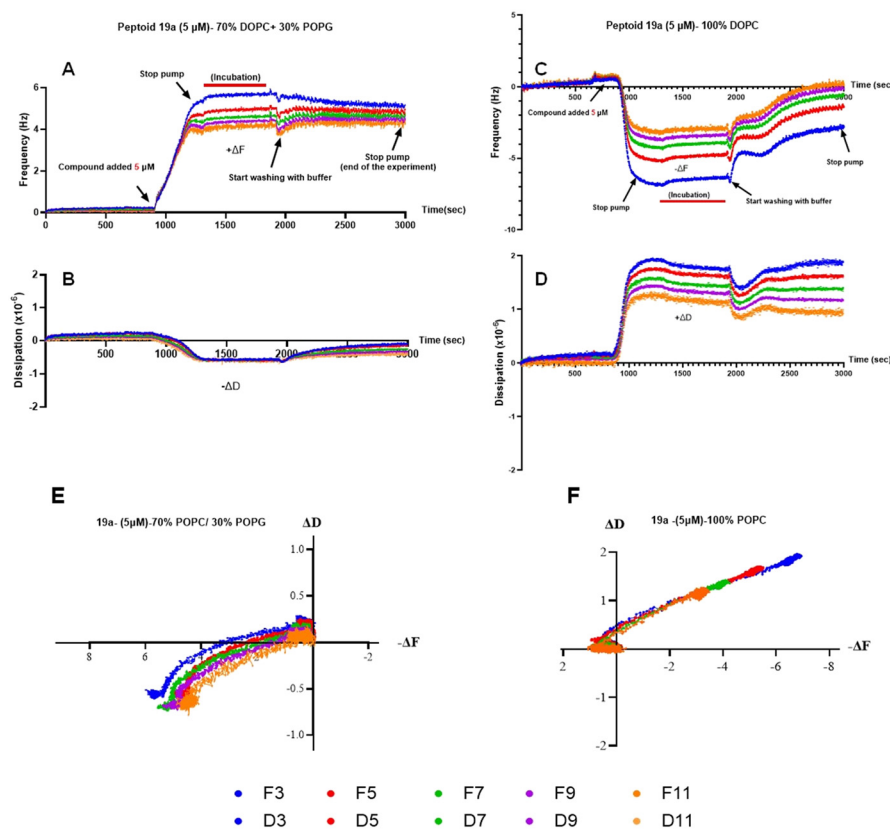
Fig. 7 Chemical structure of **19a** and **19b**.

Fig. 8 A and B) Interaction of 5 μM of **19a** with DOPC membrane, C and D) interaction of 5 μM of **19a** with 70% DOP/30% POPG membrane, E) ΔF vs. ΔD plots of 100% DOPC membrane (from the addition of **19a** to the end of incubation), F) ΔF vs. ΔD plots of 70% DOP/30% POPG membrane (from the addition of **19a** to the end of incubation).

and 30% POPG lipidic membrane can be illustrated using ΔF vs. ΔD plots.[44] Fig. 8E shows the relationship between changes in frequency and dissipation caused by the addition of **19a** on the DOPC/POPG model membrane at 5 μM. The ΔF–ΔD plot shows the loss of mass and an increase in rigidity of the membrane, indicating that compound **19a** disrupts the bacterial-type membrane, similar to the antimicrobial peptide, aurein 1.2.[45]

In contrast, Fig. 8C and D shows the effect of 5 μM **19a** on the zwitterionic phosphatidylcholine membrane (100% DOPC lipid layer), which differed from the membrane that contains a negative charge (Fig. 8A and B). Compound **19a** (5 μM) on 100% POPC caused a significant increase in mass as indicated by the negative change in frequency values ($-\Delta F$), which is most pronounced at the 3rd (-6.5 Hz) and 5th (-4.8 Hz) harmonics. These increases in the mass absorption came with a slight decrease in the rigidity of the membrane. After the wash, the mass gain was reversible, but the changes in the rigidity were not altered (Fig. 8C and D). Comparing the ΔF–ΔD plots of **19a** (5 μM) between the two membrane types makes the difference in dynamic mechanism apparent (Fig. 8E and F).

This was followed by the addition of greater concentrations of compound **19a** at 10 μM, 20 μM, and 50 μM to the same washed 100% POPC membrane. This caused a concentration

dependent increase in the mass of the membrane ($\Delta F_{3rd\ harmonic}$ = -8.6, -12.5, -17.9 Hz, respectively), combined with a decrease in the rigidity as indicated by the positive dissipation reaching its peak at 50 μM by $+5$ ppm. Additionally, **19a** exhibited dynamic resistance to removal from the POPC membrane; however, continuous washing for four times led to the removal of a small portion of it from this membrane (Fig. 9A). The ΔF–ΔD plots in Fig. 9C show this increase in both the frequency and dissipation with a high spread of the harmonics in the frequency domain and increasing spread in the dissipation domain. Especially the change in the third and fifth harmonics, which observe activity towards the surface region, suggests that tertiary amide **19a** aggregates on the POPC lipidic layer surface. A similar relationship between ΔF and ΔD was reported for peptide-Gly15Gly19-caerin1.1.[45] The addition of 5 μM of **19b** on the 100% POPC membrane showed an increase in the mass, as illustrated by a -2.7 Hz drop, and a minimal decrease in the rigidity of the 100% POPC membrane (Fig. 9B). The addition of higher concentrations of **19b** to the washed POPC membrane increased in a concentration dependent manner leading to the maximum values at 50 μM (-7.1 Hz).

After washing, the mass addition and reduction of rigidity were mostly reversible. This suggests that minimal amounts of the compound remain bound even after washing, which also introduces minimal reduction of rigidity. Interestingly,
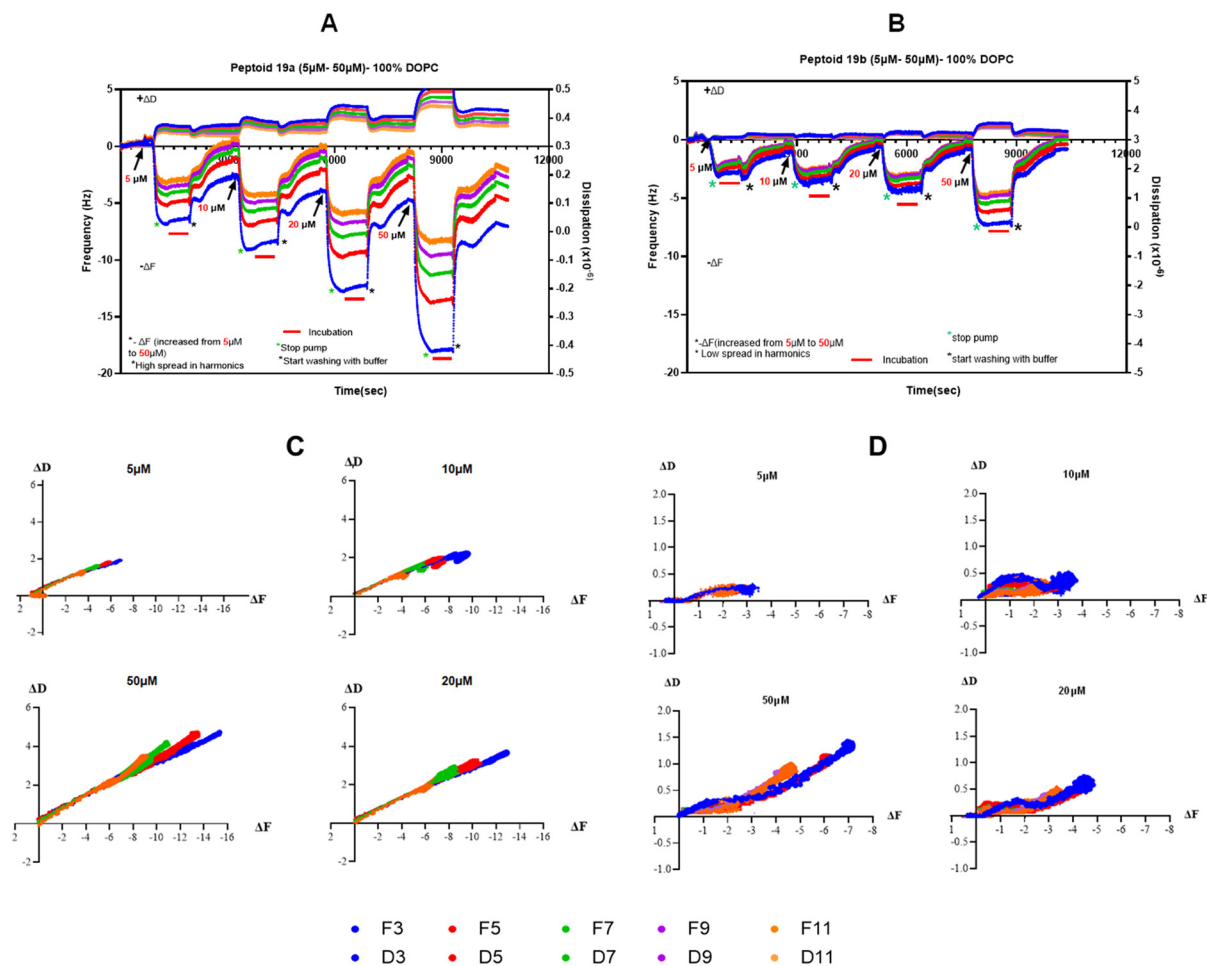
Fig. 9 A) Interaction of 5–50 μM of **19a** with 100% DOPC membrane, B) interaction of 5–50 μM of **19b** with 100% DOPC membrane, C) ΔF vs. ΔD plot of **19a** (from the addition of **19a** to the end of incubation), D) ΔF vs. ΔD plots of **19b** (from the addition of **19b** to the end of incubation).

compound **19b** (Fig. 9B) showed a similar trend as **19a** (Fig. 9A) in its effect on the 100% POPC model membrane. However, the change induced by **19b** in both frequency and dissipation as well as the spread of the harmonics is greatly reduced suggesting reduced reactivity of the compound with the membrane. The overlap between the harmonics at low concentrations of **19b** suggests that the substituted guanidino tertiary amide is penetrating the bilayer. Only at 50 μM does **19b** begin to accumulate more on the surface, whereas compound **19a** seems to aggregate largely on the surface of the bilayer at all tested concentrations (Fig. 9A). The ΔF–ΔD plots (Fig. 9C and D) show the mass increases with small changes in the rigidity, which could be a result of more pronounced binding to the surface for **19a** at all concentrations, while **19b** shows an increasing trend of insertion at low concentrations until it converts to surface binding for 50 μM.

Unlike **19a**, the addition of 5 μM **19b** (the aminohexyl guanidino tertiary amide) to the 70% POPC and 30% POPG lipidic membrane did not cause a noticeable change in mass and rigidity (Fig. 10A). The addition of 10 μM **19b** to the washed POPC and POPG membrane caused a slight increase in mass

with −1.2 Hz drop in the frequency. The mass increased as the concentration of **19b** was increased to 20 μM and 50 μM, with −2.1 Hz and −3.2 Hz changes, respectively (Fig. 10A). These increases in the mass came with small changes in dissipation and a negligible decrease in the rigidity after the wash (Fig. 10A). Interestingly, **19b** affected all the overtones of the membrane suggesting either transmembrane insertion of the substituted guanidino tertiary amide into the membrane or pore formation.[42] These results can also be observed in the ΔF–ΔD plots (Fig. 10B), where the mass increase becomes stronger with increasing concentration. Additionally, the changes in mass were reversible after washing suggesting that the **19b** can be largely removed from the membrane with only small remaining amounts of compound and effect on membrane rigidity.

Conclusion

The two guanidino sides of bromo-phenyl and dichloro-phenyl-based tertiary amides were modified by attaching one or both sides of two guanidino groups to a lipophilic tail (series **I**) (**15a–15g** and **16a–16g**) or conjugation of cationic
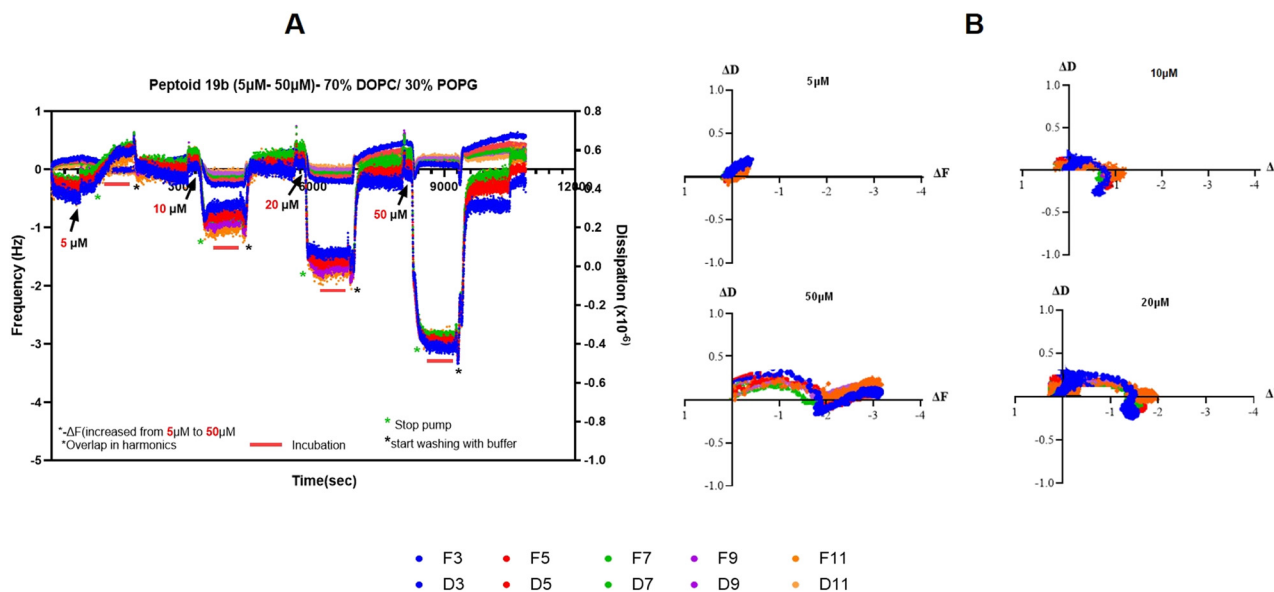
Fig. 10 A) Interaction of 5–50 μM of **19b** with 70% DOPC/30% POPG membrane, B) ΔF vs. ΔD plots for the 5–50 μM peptoid **19b** against 70% DOPC/30% POPG membrane (from the addition of **19b** to the end of incubation).

and hydrophobic groups (series **II** and **III**) (**19a–19i** and **20a–20i**). In general, the bromo-phenyl modified guanidine derivatives were slightly active compared to dichloro-phenyl ones. This work produced 70% of the modified guanidinium bromo-phenyl and dichloro-phenyl-based tertiary amides with excellent activity against *S. aureus* strains with MICs ranging from 1 μg mL^{-1} to 8 μg mL^{-1} and 50% with MICs of 4–8 μg mL^{-1} against *E. coli* strains.

The most active compound was **19a** (bromo-phenyl-based tertiary amide with phenyl and propylamine tail on the guanidine group) with MICs of 1–2 μg mL^{-1}, 4 μg mL^{-1}, and 16.5 μg mL^{-1} against *S. aureus* strains, *E. coli* strains, and *P. aeruginosa*, respectively.

In the first series, the tertiary amides bearing the shortest lipophilic tails have the highest potency against Gram-positive and Gram-negative bacteria, except *P. aeruginosa* (all the series **I** tertiary amides were inactive against *P. aeruginosa*). In series **II**, the attachment of the alkyl (3C and 6C) cationic groups with guanidine (**19a**, **20a**, **19b**, and **20b**) enhanced the activity compared to the attachment of the aryl cationic group in tertiary amides **19c** and **20c** (aniline-type). Additionally, these compounds **19a**, **20a**, **19b** and **20b** showed the best activity among all the designed compounds against all the tested strains with MIC of 1–2.3 μg mL^{-1} against *S. aureus* strains, around 4 μg mL^{-1} against *E. coli* strains, and 32–35 μg mL^{-1} against *P. aeruginosa*. In series **III**, **19i** and **20i** with a methoxy group showed the best activity against *S. aureus* and *E. coli* strains. The most active compounds of series **III** against *P. aeruginosa* were **19e** and **20e** (aniline derivatives). Most active tertiary amides disrupted between 40% to 50% of the *S. aureus* 38 biofilm and around 35% of *E. coli* K12 biofilm at their 8× MIC concentrations. The best *S. aureus* biofilm disruptor at 2×, 4×, and 8× MIC was compound **19b**, which disrupted 42%, 51%, and 75% of the

S. aureus biomass, respectively. Additionally, the most active compound against *E. coli* biofilm was **19g** with 50% disruption at 8× MIC. The membrane permeability and the QCM-D studies revealed that these modified guanidinium tertiary amides could be good bacterial cell membrane disruptors. These most active cationic tertiary amides were non-toxic against blood cells with an HC$_{50}$ of >50 μg mL^{-1}. Finally, in a comparison between previously prepared amino tertiary amides **12a** and **12b** with MICs of 11 μg mL^{-1} and 5.4 μg mL^{-1} against *S. aureus* and 11 μg mL^{-1} and 21.5 μg mL^{-1} against *E. coli*, respectively, and HC$_{50}$ of 10–20 μg mL^{-1}. In this work, a library of active compounds against *S. aureus* strains with MICs between 1–2 μg mL^{-1} and around 4 μg mL^{-1} against *E. coli*, and with the lowest toxicity against mammalian red blood cells with HC$_{50}$ of >50 μg mL^{-1} was obtained.

Author contributions

The synthesis and spectroscopic characterisation of compounds and MIC assays were conducted by G. B. The Biofilm disruption assay was conducted by G. B. The cytoplasmic membrane depolarisation assay was conducted by G. B. The haemolysis assay was conducted by G. B. The QCM-D experiment was conducted by L. H., C. G. C, and G. B. (data analysis). The manuscript was prepared by G. B. Supervision, N. K., R. K., M. W., and D. StC. B.; funding acquisition, G. B., N. K., M. W., and D. StC. B. All authors have read and agreed to the published version of the manuscript.

Conflicts of interest

The authors declare no conflict of interest.

Data availability

Supplementary information: supplementary information (SI) including the experimental section for the chemistry part, general notes, general synthesis methods, and experimental data for the designed compounds; biology data including minimum inhibitory concentration (MIC), cytoplasmic membrane permeability assay, viable cell count assay, lysis of horse red blood cells, biofilm, and QCM-D; and the compound characterization data, including NMR, VT experiment, and mass spectra is available. See DOI: https://doi.org/10.1039/D5MD00688K.

The data supporting this article have been included within the article and as part of the SI.

Acknowledgements

References

1 J. Lin, K. Nishino, M. C. Roberts, M. Tolmasky, R. I. Aminov and L. Zhang, Mechanisms of antibiotic resistance, *Front. Microbiol.*, 2015, **6**, 1–24.

2 M. S. Butler and D. L. Paterson, Antibiotics in the clinical pipeline in October 2019, *J. Antibiot.*, 2020, **73**, 329–364.

3 J. Jass and H. M. Lappin-Scott, The efficacy of antibiotics enhanced by electrical currents against Pseudomonas aeruginosa biofilms, *J. Antimicrob. Chemother.*, 1996, **38**, 987–1000.

4 R. Rathinakumar, W. F. Walkenhorst and W. C. Wimley, Broad-spectrum antimicrobial peptides by rational combinatorial design and high-throughput screening: The importance of interfacial activity, *J. Am. Chem. Soc.*, 2009, **131**, 7609–7617.

5 Y. Sang and F. Blecha, Antimicrobial peptides and bacteriocins: alternatives to traditional antibiotics, *Anim. Health Res. Rev.*, 2008, **9**, 227–235.

6 P. Kosikowska and A. Lesner, Antimicrobial peptides (AMPs) as drug candidates: a patent review (2003–2015), *Expert Opin. Ther. Pat.*, 2016, **26**, 689–702.

7 B. Mojsoska, R. N. Zuckermann and H. Jenssen, Structure-activity relationship study of novel peptoids that mimic the structure of antimicrobial peptides, *Antimicrob. Agents Chemother.*, 2015, **59**, 4112–4120.

8 D. J. Craik, D. P. Fairlie, S. Liras and D. Price, The Future of Peptide-based Drugs, *Chem. Biol. Drug Des.*, 2013, **81**, 136–147.

9 M. Won, C. Yoon, J. An, D. Kim and J. S. Kim, Mitochondria-Targeted Antibiotics toward Drug Resistant TNBC, *ACS Appl. Bio Mater.*, 2025, **8**, 7105–7112.

10 S. M. Miller, R. J. Simon, S. Ng, R. N. Zuckermann, J. M. Kerr and W. H. Moos, Comparison of the proteolytic susceptibilities of homologous L-amino acid, D-amino acid, and N-substituted glycine peptide and peptoid oligomers, *Drug Dev. Res.*, 1995, **35**, 20–32.

11 J. Stefańska, M. Antoszczak, K. Stępień, M. Bartoszcze, T. Mirski and A. Huczyński, Tertiary amides of Salinomycin: A new group of antibacterial agents against Bacillus anthracis and methicillin-resistant Staphylococcus epidermidis, *Bioorg. Med. Chem. Lett.*, 2015, **25**, 2082–2088.

12 K. Andreev, C. Bianchi, J. S. Laursen, L. Citterio, L. Hein-Kristensen, L. Gram, I. Kuzmenko, C. A. Olsen and D. Gidalevitz, Guanidino groups greatly enhance the action of antimicrobial peptidomimetics against bacterial cytoplasmic membranes, *Biochim. Biophys. Acta, Biomembr.*, 2014, **1838**, 2492–2502.

13 P. A. Wender, D. J. Mitchell, K. Pattabiraman, E. T. Pelkey, L. Steinman and J. B. Rothbard, The design, synthesis, and evaluation of molecules that enable or enhance cellular uptake: Peptoid molecular transporters, *Proc. Natl. Acad. Sci. U. S. A.*, 2000, **97**, 13003–13008.

14 H. L. Bolt and S. L. Cobb, A practical method for the synthesis of peptoids containing both lysine-type and arginine-type monomers, *Org. Biomol. Chem.*, 2016, **14**, 1211–1215.

15 W. Huang, J. Seo, J. S. Lin and A. E. Barron, Peptoid transporters: effects of cationic, amphipathic structure on their cellular uptake, *Mol. BioSyst.*, 2012, **8**, 2626–2628.

16 D. K. Kölmel, D. Fürniss, S. Susanto, A. Lauer, C. Grabher, S. Bräse and U. Schepers, Cell penetrating peptoids (CPPos): Synthesis of a small combinatorial library by using IRORI MiniKans, *Pharmaceuticals*, 2012, **5**, 1265–1281.

17 C. Y. Huang, T. Uno, J. E. Murphy, S. Lee, J. D. Hamer, J. A. Escobedo, F. E. Cohen, R. Radhakrishnan, V. Dwarki and R. N. Zuckermann, Lipitoids - Novel cationic lipids for cellular delivery of plasmid DNA in vitro, *Chem. Biol.*, 1998, **5**, 345–354.

18 Y. Su, T. Doherty, A. J. Waring, P. Ruchala and M. Hong, Roles of arginine and lysine residues in the translocation of a cell-penetrating peptide from 13C, 31P, and 19F Solid-State NMR, *Biochemistry*, 2009, **48**, 4587–4595.

19 A. Laniel, É. Marouseau, D. T. Nguyen, U. Froehlich, C. McCartney, P. L. Boudreault and C. Lavoie, Characterization of PGua4, a Guanidinium-Rich Peptoid that Delivers IgGs to the Cytosol via Macropinocytosis, *Mol. Pharmaceutics*, 2023, **20**, 1577–1590.

20 A. S. Woods and S. Ferré, Amazing stability of the arginine-phosphate electrostatic interaction, *J. Proteome Res.*, 2005, **4**, 1397–1402.

21 J. Mavri and H. J. Vogel, Ion pair formation of phosphorylated amino acids and lysine and arginine side chains: a theoretical study, *Proteins: Struct., Funct., Bioinf.*, 1996, **24**, 495–501.

22 H. L. Bolt and S. L. Cobb, A practical method for the synthesis of peptoids containing both lysine-type and arginine-type monomers, *Org. Biomol. Chem.*, 2016, **14**, 1211–1215.

23 H. L. Bolt, G. A. Eggimann, C. A. B. Jahoda, R. N. Zuckermann, G. J. Sharples and S. L. Cobb, Exploring the links between peptoid antibacterial activity and toxicity, *MedChemComm*, 2017, **8**, 886–896.

24 C. Peggion, F. Formaggio, M. Crisma, R. F. Epand, R. M. Epand and C. Toniolo, Trichogin: A paradigm for lipopeptaibols, *J. Pept. Sci.*, 2003, **9**, 679–689.

25 J. N. Steenbergen, J. Alder, G. M. Thorne and F. P. Tally, Daptomycin: A lipopeptide antibiotic for the treatment of serious Gram-positive infections, *J. Antimicrob. Chemother.*, 2005, **55**, 283–288.

26 H. Tsubery, I. Ofek, S. Cohen and M. Fridkin, N-terminal modifications of Polymyxin B nonapeptide and their effect on antibacterial activity, *Peptides*, 2001, **22**, 1675–1681.

27 R. M. Green and K. L. Bicker, Evaluation of peptoid mimics of short, lipophilic peptide antimicrobials, *Int. J. Antimicrob. Agents*, 2020, **56**, 106048.

28 N. P. Chongsiriwatana, T. M. Miller, M. Wetzler, S. Vakulenko, A. J. Karlsson, S. P. Palecek, S. Mobashery and A. E. Barron, Short alkylated peptoid mimics of antimicrobial lipopeptides, *Antimicrob. Agents Chemother.*, 2011, **55**, 417–420.

29 R. Kapoor, M. W. Wadman, M. T. Dohm, A. M. Czyzewski, A. M. Spormann and A. E. Barron, Antimicrobial peptoids are effective against Pseudomonas aeruginosa biofilms, *Antimicrob. Agents Chemother.*, 2011, **55**, 3054–3057.

30 J. S. Lin, L. A. Bekale, N. Molchanova, J. E. Nielsen, M. Wright, B. Bacacao, G. Diamond, H. Jenssen, P. L. Santa Maria and A. E. Barron, Anti-persister and Anti-biofilm Activity of Self-Assembled Antimicrobial Peptoid Ellipsoidal Micelles, *ACS Infect. Dis.*, 2022, **8**, 1823–1830.

31 J. Hoque, M. M. Konai, S. S. Sequeira, S. Samaddar and J. Haldar, Antibacterial and Antibiofilm Activity of Cationic Small Molecules with Spatial Positioning of Hydrophobicity: An in Vitro and in Vivo Evaluation, *J. Med. Chem.*, 2016, **59**, 10750–10762.

32 G. Bahatheg, R. Kuppusamy, M. Yasir, S. K. Mishra, D. S. C. Black, M. Willcox and N. Kumar, Functionalized Phenyl Peptoids with Enhanced Antibacterial Potency, *ACS Infect. Dis.*, 2025, **11**, 1648–1661.

33 G. Bahatheg, R. Kuppusamy, M. Yasir, S. Bridge, S. K. Mishra, C. G. Cranfield, D. StC. Black, M. Willcox and N. Kumar, Dimeric peptoids as antibacterial agents, *Bioorg. Chem.*, 2024, **147**, 107334.

34 R. Kuppusamy, M. Yasir, T. Berry, C. G. Cranfield, S. Nizalapur, E. Yee, O. Kimyon, A. Taunk, K. K. K. Ho, B. Cornell, M. Manefield, M. Willcox, D. S. C. Black and N. Kumar, Design and synthesis of short amphiphilic cationic peptidomimetics based on biphenyl backbone as antibacterial agents, *Eur. J. Med. Chem.*, 2018, **143**, 1702–1722.

35 Y. Ge, D. L. MacDonald, K. J. Holroyd, C. Thornsberry, H. Wexler and M. Zasloff, In vitro antibacterial properties of pexiganan, an analog of magainin, *Antimicrob. Agents Chemother.*, 1999, **43**, 782–788.

36 P. C. Fuchs, A. L. Barry and S. D. Brown, In vitro antimicrobial activity of MSI-78, a magainin analog, *Antimicrob. Agents Chemother.*, 1998, **42**, 1213–1216.

37 N. P. Chongsiriwatana, J. A. Patch, A. M. Czyzewski, M. T. Dohm, A. Ivankin, D. Gidalevitz, R. N. Zuckermann and A. E. Barron, Peptoids that mimic the structure, function, and mechanism of helical antimicrobial peptides, *Proc. Natl. Acad. Sci. U. S. A.*, 2008, **105**, 2794–2799.

38 H. Cohen, N. A. Wani, D. Ben Hur, L. Migliolo, M. H. Cardoso, Z. Porat, E. Shimoni, O. L. Franco and Y. Shai, Interaction of Pexiganan (MSI-78)-Derived Analogues Reduces Inflammation and TLR4-Mediated Cytokine Secretion: A Comparative Study, *ACS Omega*, 2023, **8**, 17856–17868.

39 B. Amorena, E. Gracia, M. Monzón, J. Leiva, C. Oteiza, M. Pérez, J. L. Alabart and J. Hernández-Yago, Antibiotic susceptibility assay for Staphylococcus aureus in biofilms developed in vitro, *J. Antimicrob. Chemother.*, 1999, **44**, 43–55.

40 R. M. Donlan and J. W. Costerton, Biofilms: Survival mechanisms of clinically relevant microorganisms, *Clin. Microbiol. Rev.*, 2002, **15**, 167–193.

41 T. Bjarnsholt, O. Ciofu, S. Molin, M. Givskov and N. Høiby, Applying insights from biofilm biology to drug development-can a new approach be developed?, *Nat. Rev. Drug Discovery*, 2013, **12**, 791–808.

42 T. John, B. Abel and L. L. Martin, The Quartz Crystal Microbalance with Dissipation Monitoring (QCM-D) Technique Applied to the Study of Membrane-Active Peptides, *Aust. J. Chem.*, 2018, **71**, 543–546.

43 A. Mechler, S. Praporski, K. Atmuri, M. Boland, F. Separovic and L. L. Martin, Specific and selective peptide-membrane interactions revealed using quartz crystal microbalance, *Biophys. J.*, 2007, **93**, 3907–3916.

44 K. F. Wang, R. Nagarajan and T. A. Camesano, Differentiating antimicrobial peptides interacting with lipid bilayer: Molecular signatures derived from quartz crystal microbalance with dissipation monitoring, *Biophys. Chem.*, 2015, **196**, 53–67.

45 G. A. McCubbin, S. Praporski, S. Piantavigna, D. Knappe, R. Hoffmann, J. H. Bowie, F. Separovic and L. L. Martin, QCM-D fingerprinting of membrane-active peptides, *Eur. Biophys. J.*, 2011, **40**, 437–446.